Creep failure Model of a 9Cr1Mo-NbV (P91) steel integrating multiple deformation and damage mechanisms

V. Gaffard, J. Besson, A.F. Gourgues-Lorenzon

Ecole des Mines de Paris, Centre des Matériaux, UMR CNRS 7633

BP 87 91003 Evry Cedex France

vincent.gaffard@ensmp.fr, jacques.besson@ensmp.fr, anne-francoise.gourgues@ensmp.fr

Abstract

P91 tempered martensitic stainless steels have recently been developed for boilers and turbines of supercritical and ultra supercritical power plants. Under creep loading conditions at high temperature, those steels exhibit changes in creep flow and damage mechanisms depending on the stress level. Several creep flow and damage mechanisms may also be simultaneously activated.

The aim of this contribution is to present a new model integrating a coupling between constitutive equations and damage evolution, and considering multiple viscoplastic deformation mechanisms.

The model formulation is first introduced. It is then applied to model creep flow and damage of a tempered martensitic stainless steel at 625°C for which creep tests on several kinds of specimen geometry were carried out.

1. Description of the model

1.1. Description of creep flow in the damage free material

At high temperature, creep flow proceeds by two main mechanisms i.e. by dislocation cross-slip or climb at high stresses and by grain boundary diffusion at low stresses. Therefore, the model was designed to describe these two mechanisms. An additive decomposition was chosen and the resulting strain rate tensor, is given by :

$$\underline{\dot{\varepsilon}} = \underline{\dot{\varepsilon}}_e + \underline{\dot{\varepsilon}}_{vp} + \underline{\dot{\varepsilon}}_d \tag{1}$$

where $\underline{\dot{\varepsilon}}_e$ is the elastic strain rate tensor, $\underline{\dot{\varepsilon}}_{vp}$ accounts for power-law creep and $\underline{\dot{\varepsilon}}_d$ accounts for low stress grain boundary diffusion creep. The corresponding subscripts vp and d will be used to designate these two mechanisms in the following.

For each mechanism (m = vp, d), the viscoplastic equivalent strain rate $\dot{p}_n$ is given by a Norton law :

$$\dot{p}_m = \left\langle \frac{\phi_m}{K_m} \right\rangle^{n_m} \text{ if } \phi_m > 0 \text{ and } \dot{p}_m = 0 \text{ otherwise} \tag{2}$$

where $\phi_m = \sigma^*_m - R_m$ describes the viscoplastic equipotential surface. R_m is the flow stress which is expressed as a function of p_m. σ^*_m is an effective scalar stress which is equal to the von Mises stress, σ_{eq}, for the undamaged material. The strain rate tensor, $\dot{\underline{\varepsilon}}_m$, is given by the normality rule :

$$\dot{\underline{\varepsilon}}_m = \dot{p}_m \cdot \frac{\partial \phi_m}{\partial \underline{\sigma}} \tag{3}$$

1.2. Coupling damage and creep flow

Coupling between creep flow and damage properties is based on the mechanics of porous media (Besson and al (2001)). An effective stress σ^*_m depending on damage is defined following the description of the Gurson Tvergaard Needleman (GTN) model (1984) :

$$\frac{\sigma^2_{eq}}{\sigma^{*2}_m} + 2q_1 f^* \cosh\left(\frac{q_2}{2} \frac{\sigma_{kk}}{\sigma^*_m}\right) - 1 - q_1^2 f^{*2} \overset{\text{def.}\sigma^*_m}{=} 0 \tag{4}$$

where q_1 and q_2 are model parameters, and f^* is a function of the porosity f which is defined by $f^* = f$ if $f < f_c$ and $f^* = f_c + \delta.(f - f_c)$ if $f > f_c$ to account for cavity coalescence in the later stage of the material creep life.

Values of f_c and δ were set to respectively 0.1 and 5.0. For the "d" mechanism, no coarsening law was defined so that fracture occurs for $f_{td} = 1/q_1 = 0.666$.

The strain rate tensor is modified to be :

$$\dot{\underline{\varepsilon}}_m = (1-f)\dot{p}_m \frac{\partial \phi_m}{\partial \underline{\sigma}} \text{ so that } (1-f)\dot{p}_m \sigma^*_m = \dot{\underline{\varepsilon}}_m : \underline{\sigma} \tag{5}$$

The evolution of porosity is expressed using mass conservation and taking into account the nucleation of new voids:

$$\dot{f} = (1-f)\sum_m \text{trace}(\dot{\underline{\varepsilon}}_m) + \dot{f}_n = (1-f)^2 \sum_m \dot{p}_m \text{ trace}\left(\frac{\partial \phi_m}{\partial \underline{\sigma}}\right) + \dot{f}_n \text{ with } \dot{f}_n = \sum_m \dot{f}_{nm} \tag{6}$$

As the stress triaxiality ratio may play a key role in the nucleation kinetics, for each mechanism, the kinetics of nucleation was described by

$$\dot{f}_{nm} = \left(A_m + B_m \left(\frac{1}{3}\frac{\sigma_{kk}}{\sigma_{eq}}\right)^{\alpha_m}\right)\dot{p}_m \tag{7}$$

where $\tau = \frac{1}{3}\frac{\sigma_{kk}}{\sigma_{eq}}$ is the stress triaxiality ratio, A_m, B_m and α_m are adjustable parameters.

2. Modelling creep flow and damage behaviour of a 9Cr-1MoNbV (P91) steel

2.1. Material and experiments

The material of the study is a tempered chromium martensitic stainless steel whose chemical composition is given in table 1. It was supplied as a pipe of 295 mm in outer diameter and 55 mm in thickness.

For experimental studies, all specimens were machined along the longitudinal axis of the pipe. All experiments were carried out at 625°C.

C	Si	Mn	P	S	Al	Cr	Ni	Mo	V	Nb	N
0.09	0.31	0.41	0.014	0.005	0.016	8.56	0.26	0.92	0.21	0.065	0.042

TABLE 1 : Chemical composition of the steel studied in wt%

Tension creep tests were carried out on smooth bars and various kinds of notched bars. Smooth round tensile bars (SC) have a gauge length of 36 mm and gauge diameter of 5 mm. These tests are part of the HIDA project (Prunier et al (1998)); round U-notched bars (NC1.2 and NC4.0) have a maximum diameter of 13 mm and a minimum diameter of 6 mm with a notch radius of 1.2 and 4.0 mm respectively and round V-notched bars (NC0.25) have a maximum diameter of 23 mm and a minimum diameter of 14 mm with a notch radius of 0.25 mm. Elongation of NC0.25, 1.2 and 4.0 specimens was measured between points located on both sides of the notched area with gauge lengths of respectively 10 mm, 20 mm and 20 mm. Tensile creep tests were carried out under constant applied load in controlled laboratory atmosphere (20°C ± 2°C and 50% relative humidity). The load was applied using dead weights for SC specimens and using an electrical mechanical testing machine for NC0.25, 1.2 and 4.0 specimens. The temperature was monitored using three thermocouples spot welded onto the specimen surface. The temperature gradient between top and bottom ends of the specimen did not exceed 2°C. The elongation measured using Linear Variable Differential Transducers was continuously recorded with a sensitivity of 1 µm.

2.2. Creep flow and damage properties

First, experiments on SC specimens (see figure 1) were used to determine the stress dependence of the steady state creep strain rate by assuming a usual Norton law : $\dot{\varepsilon}_{ss} = B\sigma^n$. The plot corresponding to experimental data leads to the determination of a Norton exponent of 8. This result suggests that deformation is accomodated by dislocation climb or cross slip in the explored stress domain.

Similar data were plotted from Kloc and Sklenicka (1997) for the low stress creep regime. A Norton exponent of 1 was found corresponding to a creep regime where deformation is accomodated by grain boundary diffusion. Therefore, two main creep regimes can be distinguished depending on the applied engineering stress σ_n : the high stress creep regime for $\sigma_n > 70$ MPa and the low stress creep regime for $\sigma_n < 70$ MPa.
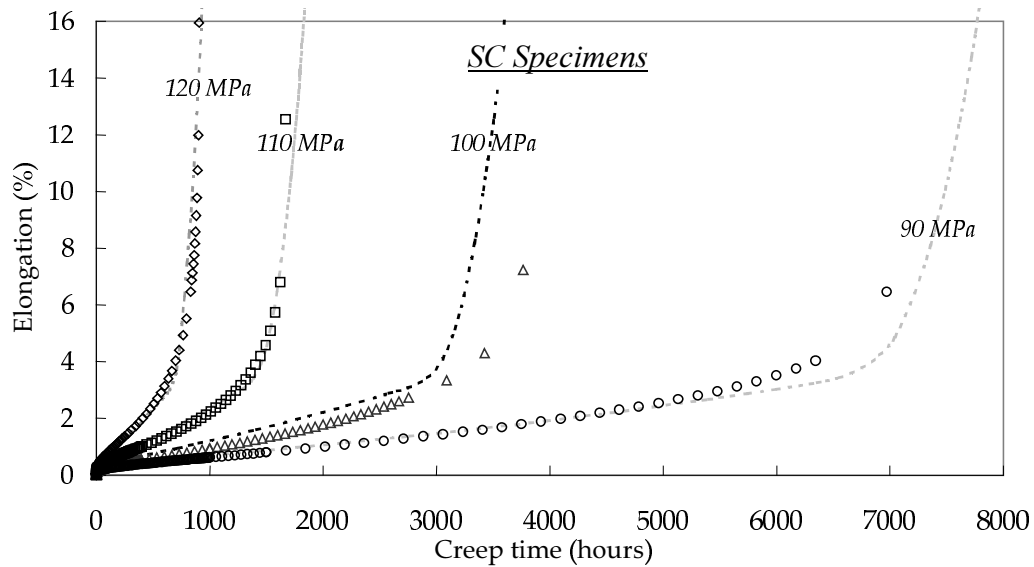
FIGURE 1 : Comparisons of experimental (symbols) and calculated (lines)
creep curves for creep tests on SC specimens

Experiments on NC specimens (see figure 2 for NC1.2 specimens) were carried out to investigate the effect of the stress triaxiality ratio on damage nucleation and growth kinetics. Moreover, NC1.2 and NC4.0 specimens were machined with respectively three and two widely separated notches in order to investigate damage mechanisms. This allowed metallographic study of longitudinal cross-sections of non broken notches which were assumed to be representative of the damage state at the onset of the tertiary stage (Piques (1986)).
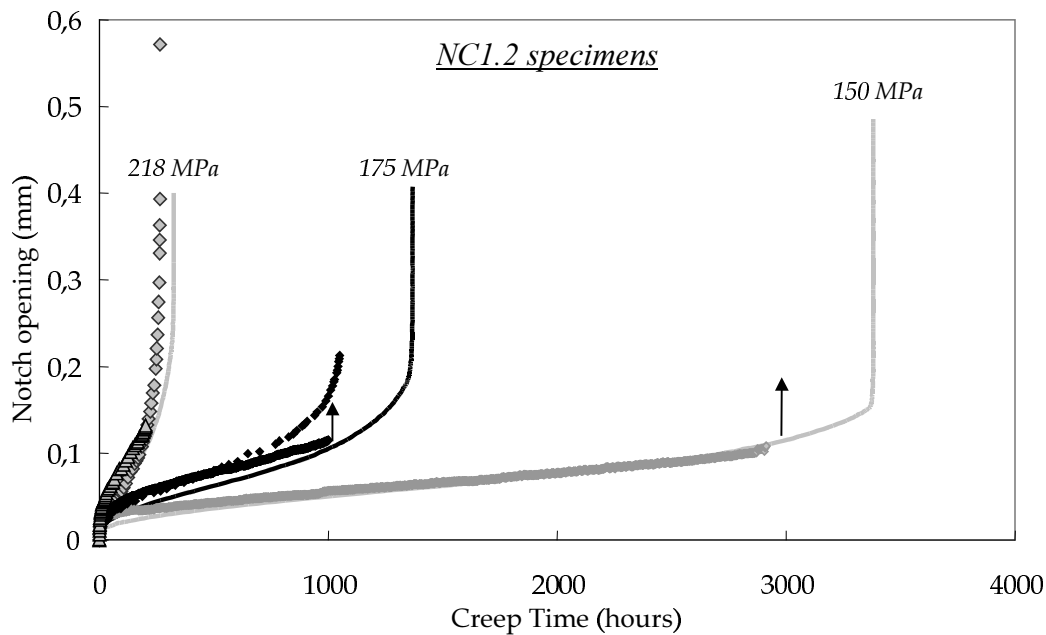

FIGURE 2 : Comparison of experimental (symbols) and calculated (lines) creep curves for
creep tests on NC1.2 specimens

Cavitation processes were investigated both on fracture surface and on polished cross sections of the specimens. Observation of non oxidised fracture surface show that the overall fracture mode is almost ductile. However, as evidenced in figure 3b, the fracture mode of the steel can be described as "intergranular then ductile", as, fracture starts from intergranular cavitation at subgrains boundaries and then develops by growth and coalescence of cavities in a ductile manner.
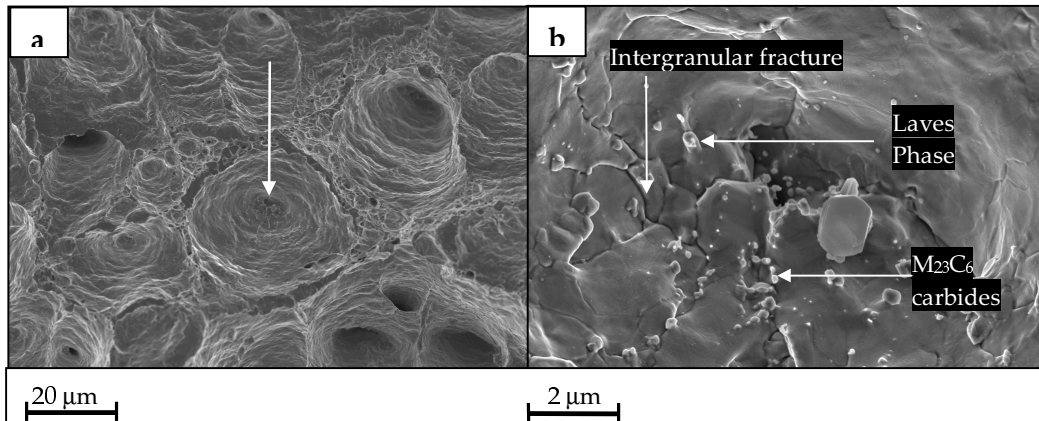

FIGURE 3 : Fracture surface of a creep specimen tested under vacuum (120MPa – 1800 hours)- SEM observations (a) . General view (b). Closer view of the dimple (arrow in (a))

The investigations on cross sections evidenced the presence of such small grain resulting from lath martensite recovery. In fact the softening of the initial lath structure largely promotes the high increase in the strain rate in the tertiary stage (Kadoya et al (1997)) and in particular triggers necking of SC specimens. Morphology and location of cavities were also observed. It was observed that the cavitation process mainly occurred by nucleation of small voids at grain boundaries. Elongated cavities resulting from the coarsening of small round voids were often observed. Surface porosity ratio were measured and location of rupture starting area could be determined (see figure 4).
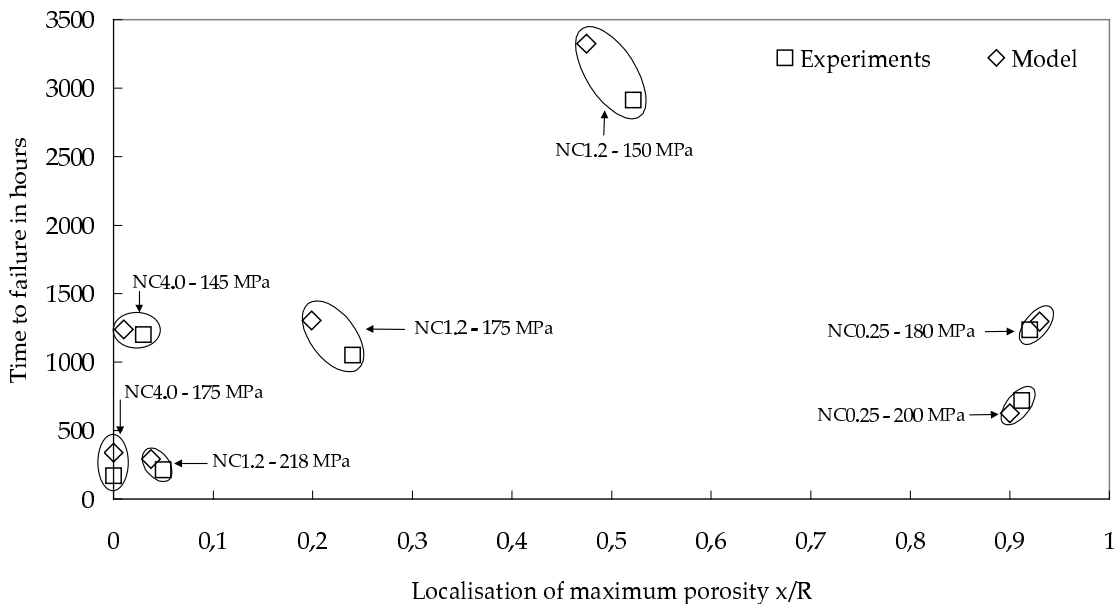
FIGURE 4 : Damage location for NC1.2 and NC0.25 specimens
Comparison between model predictions and experimental observations

It was also shown that damage is very low at the beginning of the tertiary creep stage and from the study on notched specimens, that cavitation is largely promoted by high stress triaxiality ratios.

2.3. Creep fracture properties

All results on SC specimens were represented in a "nominal stress versus time to failure" plot (see figure 4). Results from Kimura et al (2000) were added. Using experimental data, Monkman- Grant constant and Larson-Miller parameters were evaluated. Predictions of creep time to failure given by the Larson Miller parameter are given in figure 5.
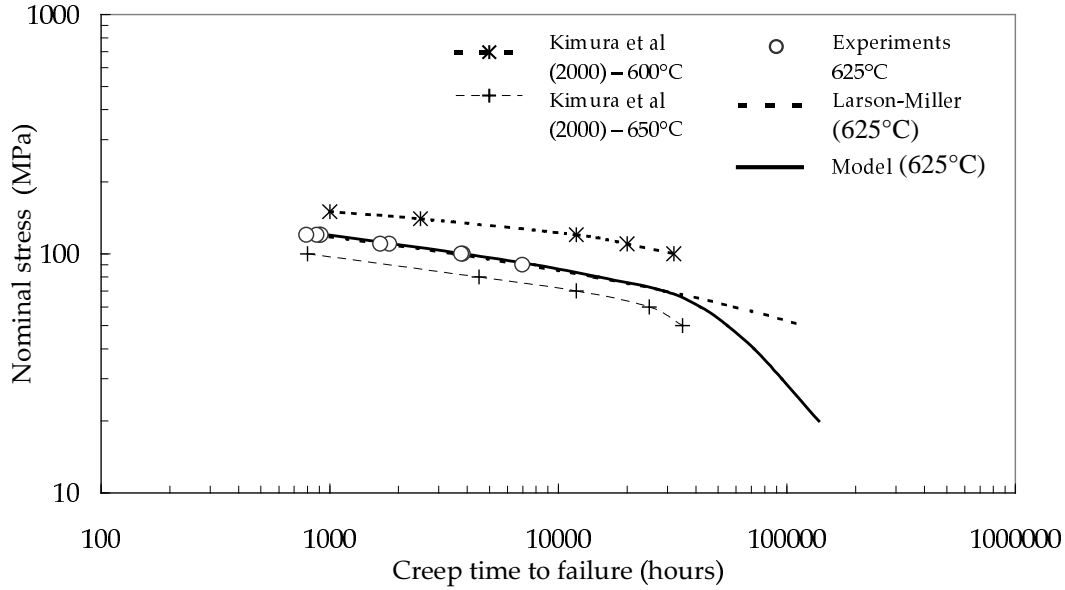

FIGURE 5 : Stress versus time to failure for SC specimens

2.4. Identification of the model parameters

The model was implemented in the FE software Zebulon (Besson and Foerch (1997)) to perform simulations of test specimens. Calculations were performed using square elements (quadratic interpolation reduced integration) of 100 μm in size for all specimens. The model parameters were identified using an inverse analysis approach.

No significant damage could be detected in the steady state creep regime. Therefore, creep flow properties were determined without accounting for coupling with damage (model introduced in section 1.1).

Yield stress term in the viscoplastic creep regime "vp" was designed to account for material softening so that :

$$R_{vp}(p_{vp}) = R_{ovp} + Q_{vp1}(1-\exp(-b_{vp1} \, p_{vp})) - \left\{ Q_{vp2}(1-\exp(-b_{vp2}(p_{vp}-p_c))) \right\} (p_{vp} > p_c)$$

where $R_{ovp} + Q_{vp1}(1-\exp(-b_{vp1} \, p_{vp}))$ represents material hardening in the first steps of creep deformation and $Q_{vp2}(1-\exp(-b_{vp2}(\bar{p}_{vp}-p_c)))$ is the softening function which is only effective for equivalent viscoplastic strain larger than $p_c = 0.03$. This critical strain p_c corresponding to the onset of softening effects was set because influence of softening on creep flow properties

should only appear after dislocation rearrangement and after dislocation annihilation overrides dislocation production. The yield stress function was set to : $R_{m,d}(\bar{p}_d) = 0$ for the diffusional mechanism as it was assumed that no significant hardening of the material is involved by diffusion at grain boundary.

The resulting set of parameters describing creep flow at 625°C is given in table 2.

Young's modulus	E	145 GPa
Poisson's ratio	υ	0.3
Viscoplastic hardening at 625°C	R_{0vp}	0 MPa
	Q_{vp1}	40 MPa
	b_{vp1}	569
	Q_{vp2}	40 MPa
	b_{vp2}	75
	p_c	0.03
Viscoplastic strain rate at 625°C	K_{vp}	542 MPa.h$^{-1/nvp}$
	n_{vp}	5.4
Diffusion strain rate at 625°C	K_d	0.33 10^9 MPa.h$^{-1/nd}$
	n_d	1.0

TABLE 2 : Creep flow parameters

Then attention was focused on determining damage parameters using the fully coupled model (see section 1.2). First, q_1 and q_2 were fixed to their classical values i.e. $q_1 = 1.5$ and $q_2 = 1.0$. The works of McLean (1981) and Myers (1987) gave arguments to set $\alpha_{vp} = \alpha_d = 2.0$. Advantages were taken from the diversity of the experimental database. The parameters A_{vp} and A_d which give the dependence of the nucleation kinetics to the overall strain were fitted on to represent the creep tertiary stage for SC specimens. Then, parameters B_{vp} and $B_{d,}$ which give the dependence of the nucleation kinetics to the stress triaxiality ratio were fitted to represent the creep tertiary stage for NC specimens. The resulting set of parameters is given in table 3.

GTN model	q_1	1.5
	q_2	1.0
	f_c	0.1
	δ	5.0
Nucleation by viscoplastic deformation	A_{vp}	0.01
	B_{vp}	0.15
	α_{vp}	2.0
Nucleation by diffusional deformation	A_d	12
	B_d	15
	α_d	2.0

TABLE 3: Creep damage parameters

2.4. Validation of the model

The model was found to well reproduce creep curves (i.e. the three creep stages and the time to failure) for all specimens (see figure 1 for SC specimens creep curves, figure 2 for NC1.2 specimens creep curves and figure 5 for time to failure).

The numerical calculations were also used to determine the rupture location in notched specimens for various stress levels. The results given in figure 4 show that the model well predicts rupture location which gives arguments to state that effects of stress triaxiality ratio on nucleation kinetics are well taken into account.

Finally, the model is able to predict premature creep time to failure which should be observed beyond 30000 hours (see figure 5). Those results are in accordance with Kimura et al (2000) but experimental data for longer tests duration would give more arguments to test the model validity.

Conclusions

The main results of the work presented in this paper are :
1. Creep tests on various kinds of specimens geometry were performed on a tempered P91 type martensitic stainless steel at 625°C (898°K) and give experimental data on the material creep flow properties in the high stress creep regime. Results from Kloc and Sklenicka (1997) were added to the database to describe the low stress creep regime.
2. A model including constitutive equations to represent all creep mechanisms and a coupling between flow and damage contributions was designed in the framework of continuum damage mechanics of porous media.
3. Constitutive equations were designed to take softening effects into account.
4. All damage stages i.e. nucleation, growth and coarsening of cavities as well as their dependence to the stress triaxiality and the equivalent viscoplastic strain were represented.
5. The resulting model well reproduced the experimental results from high to low stresses and is able to predict long term premature failure.

References
1. Besson J., Steglich D., Brocks W. *International Journal of Solids and Structures*.8259-8284. 2001.
2. Besson J., Foerch R., *Computations Methods Applied to Mechanical Engineering.* **142**, 165-187,1997
3. Kadoya Y., Nishimura N., Dyson B.F. and McLean M., *Creep and Fracture of Engineering Materials and Structures.* Edited by J.C.Earthman and F.A. Mohamed. The Minerals Metals and Materials Society, 1997
4. Kimura K., Kushima H., Abe F., *Key Engineering Materials (Switzerland).* **171-174**, 461-468, 2000
5. Tvergaard V., Needleman A., *Journal of Mechanics Physics Solids,* **32**, 373-393, 1984
6. Kloc L. , Scklenicka V. , *Materials Science Engineering*, **A272,** 272-299, 1997
7. McLean M. (1981). *Annales de chimie françaises*. **6**.124-139.
8. Myers M.R., Pilkington R., Needham N.G. (1987). *Materials Science and Engineering.* **95(2)**. 81-91.
9. Piques R. *PhD Thesis – Ecole Nationale Supérieure des Mines de Paris* (1986).
10. Prunier V., Gampe U., Nikbin K., Shibli I.A. *Creep and fatigue crack growth in high temperature plant.* HIDA Conference - CEA Saclay – France. 1998.
11. Tvergaard V. , *Advances in Applied Mechanics*, **27**, 83-151, 1989.